Biosensors and Bioelectronics 53 (2014) 406–413

Contents lists available at ScienceDirect

Biosensors and Bioelectronics

journal homepage: www.elsevier.com/locate/bios

Label-free detection of endocrine disrupting chemicals by integrating a competitive binding assay with a piezoelectric ceramic resonator

Liang-sheng Hu [a,b], Chi-Chun Fong [a,b], Lan Zou [a], Wing-Leung Wong [c], Kwok-Yin Wong [c], Rudolf S.S. Wu [d], Mengsu Yang [a,b,*]

[a] Key Laboratory of Biochip Technology, Shenzhen Biotech and Health Centre, City University of Hong Kong, Shenzhen 518057, PR China
[b] Department of Biology and Chemistry, and the State Key Laboratory of Marine Pollution, City University of Hong Kong, 83 Tat Chee Avenue, Kowloon, Hong Kong, PR China
[c] Department of Applied Biology and Chemical Technology, and the State Key Laboratory of Chirosciences, The Hong Kong Polytechnic University, Hung Hom, Kowloon, Hong Kong, PR China
[d] School of Biological Science, The University of Hong Kong, Hong Kong, PR China

ARTICLE INFO

Article history:
Received 11 July 2013
Received in revised form
26 September 2013
Accepted 27 September 2013
Available online 9 October 2013

Keywords:
Piezoelectric ceramic biosensor
Endocrine disrupting chemicals
Nanoparticle

ABSTRACT

A piezoelectric biosensor for detection of endocrine disrupting chemicals (EDCs) was developed by incorporating chemical/biochemical recognition elements on the ceramic resonator surface for competitive binding assays. A facile electrodeposition was employed to modify the sensor surface with Au nanoparticles, which increased the surface area and enhanced the binding capacity of the immobilized probes. Thiol-labeled long chain hydrocarbon with bisphenol A (BPA) as head group was synthesized and self-assembled on the Au nanoparticle surface as the sensing probes, which showed a linear response upon the binding of estrogen receptor (ER-α) ranging from 1 to 30 nM. Detection of estrone, 17β-estradiol and BPA was achieved by integrating a competitive binding assay with the piezoelectric sensor. In this detection scheme, different concentrations of EDCs were incubated with 30 nM of ER-α, and the un-bounded ER-α in the solution was captured by the probes immobilized on the ceramic resonator, which resulted in the frequency changes for different EDCs. The biosensor assay exhibited a linear response to EDCs with a low detection limit of 2.4–2.9 nM ($S/N=3$), and required only a small volume of sample (1.5 μl) with the assay time of 2 h. The performance of the biosensor assay was also evaluated for rapid and facile determination of EDCs of environmental relevant concentrations in drinking water and seawater, and the recovery rate was in the range between 94.7% and 109.8%.

1. Introduction

Over the past decades, increasing scientific and public attention has been focused on endocrine disrupting chemicals (EDCs) because they are able to mimic or antagonize the effects of endogenous hormones, such as estrogens and androgens (Krishnan et al., 1993; Tabb and Blumberg, 2006), and influence the central nervous system as well as the reproductive system in human and wildlife (Colborn et al., 1993; Waring and Harris, 2005). The definition of EDCs has been extended to include a wide class of chemicals from natural and synthetic estrogens and androgens to industrial chemicals (Fang et al., 2003; Liu et al., 2009). Among these, estrogens such as estrone (E1), 17β-estradiol (E2), estriol (E3) and bisphenol A (2, 2-bis (4-hydroxyphenol) propane, BPA) are the main EDCs which have been found in rivers, seawaters and even tap waters (Diamanti-Kandarakis et al., 2009). Many studies suggested that chronic, low-level exposure to endocrine disruptors might cause adverse biological effects in animals including human (Damgaard et al., 2002; Diamanti-Kandarakis et al., 2009; Tsutsumi, 2005). Therefore, in order to ensure drinking water safety and protect local ecosystems, there is an urgent need among research community, government and industries to develop sensitive analytical tools to monitor these hazardous chemicals.

One of the EDCs, BPA, is an essential monomer for the production of high quality food packing materials, such as epoxy coating and polycarbonate plastic (Ash and Ash, 2005; Vandenberg et al., 2007,2010). BPA is found in numerous consumer products, including baby bottles, reusable water bottles, reusable food containers, as well as in lacquers coating metal products such as water supply pipes (Vandenberg et al., 2007,2010). Long-term BPA exposure has been associated with reproductive disorders including decline in sperm counts, birth defects because fetal exposure, increased incidence of infertility, genital tract abnormalities, obesity, attention deficit hyperactivity, and prostate and breast cancer (Delbes et al., 2006; Hamid and Eskicioglu, 2012; McLachlan et al., 2006). E1 and E2 are two

* Corresponding author. Tel.: +852 3442 7797; fax: +852 3442 0552.
E-mail address: bhmyang@cityu.edu.hk (M. Yang).

0956-5663/$ - see front matter © 2013 Elsevier B.V. All rights reserved.
http://dx.doi.org/10.1016/j.bios.2013.09.068

kinds of naturally produced estrogens that are mainly derived from excreta of humans and livestock, and 16α-hydroxyestrone is the hepatic metabolite of the natural estrone by 16α-hydroxylation pathway (Hamid and Eskicioglu, 2012). E1 and E2 are known to be carcinogenic for human females that may also cause breast pain, nausea, headache, hypertension, and leg cramps (Ahmed et al., 2002; Hamid and Eskicioglu, 2012).

Since EDCs are present in extremely low concentration level (e.g., <0.1–$56\ ng\ L^{-1}$ E1; 0.2–$141\ ng\ L^{-1}$ E2) in the environment (Gomes and Lester, 2002), one of the main challenges for research is to develop sensitive and accurate methods for determination of these chemicals. Laboratory-based techniques, such as gas chromatography–mass spectrometry (GC–MS) (Lu et al., 2013; Meesters and Schroder, 2002; Patil et al., 2011), liquid chromatography coupled with mass spectrometry (LC–MS) (Di Carro et al., 2010; Magi et al., 2010), liquid chromatography with electrochemical detection (LC–ED) (D'Antuono et al., 2001), and high performance liquid chromatography (HPLC) (Lin et al., 2011) are commonly used for detection of EDCs, in particular BPA. These methods are highly sensitive and specific but also expensive, time-consuming, and require skilled operators and laborious pre-treatment such as pre-concentration and extraction stages, and thus do not allow for point-of-care detection and rapid processing of samples.

Immunoassays have been widely used as an alternative to traditional chromatographic methods for environmental analysis, which are highly sensitive and specific to the target chemical or group of chemicals. To date, different kinds of immunosensors for detection of EDCs have been reported, such as enzyme-linked immunosorbent assays based on surface plasmon resonance (Gutierrez-Gallego et al., 2009; Marchesini et al., 2005; Matsumoto et al., 2005) and total internal reflection fluorescence (Rodriguez-Mozaz et al., 2005; Tschmelak et al., 2004). Impedimetric (Rahman et al., 2007) and potentiometric (Piao et al., 2008) immunosensors were developed by using polyclonal antibodies coupled with conducting polymers. Monoclonal antibody conjugated magnetic particles were used as pre-concentration and signal generating elements in immunoassay systems (Matsunaga et al., 2003; Piao et al., 2008; Tanaka et al., 2004; Xu et al., 2012). Although the above immunosensors can selectively and sensitively detect EDCs, most of the methods are relatively expensive due to large amount of enzyme or antibody needed during testing. Therefore, it is important to develop a simple, efficient, cost-effective, and sensitive analytical tool for the determination of trace amounts of EDCs in the environment.

We have previously developed a novel piezoelectric biosensor using lead zirconium titanate (PZT) ceramic resonator as the transducer for label-free, cost-effective, and direct detection of cancer biomarkers (Su et al., 2013). The biosensor device showed high sensitivity and fast detection with small amount of sample (1 μl). Since the signal of the sensor platform depends on surface mass changes of the transducer, it is difficult to detect the small molecular weight EDCs directly using the immunosensor format. In this study, we developed a label-free biosensor for model EDCs including E1, E2 and BPA by integrating a competitive binding assay with the piezoelectric ceramic sensor modified with specific probes. Our study demonstrated that the piezoelectric ceramic biosensor assay may be used for rapid and sensitive detection of EDCs in environmental samples.

2. Experimental

2.1. Chemicals

The standards of BPA, E1, E2, chloroauric acid ($HAuCl_4 \cdot H_2O$), $K_3[Fe(CN)_6]$, $K_4[Fe(CN)_6]$, KCl, NaH_2PO_4 and Na_2HPO_4, H_3PO_4, NaOH, hydroquinone (HDQ), o-bromophenol (2-BRP), 2,2′,4,4′-tetrabromodiphenyl ether (PBDE-47), bovine serum albumin (BSA), 6-mercaptohexanol (MCH), 11-mercapto-1-undecanol (MUD), 11-mercaptoundecanoic acid, *tert*-butyl(chloro)diphenylsilane, acetonitrile, bromine-dichloromethane, dichloromethane, tetra-butylammonium fluoride were purchased from Sigma Chemical Co. (St Louis, MO). Recombinant human estrogen related receptor alpha (ER-α) ligand binding domain was obtained from Life technologies Co. The phosphate buffer solution (PBS, 0.1 M) was prepared by dissolving NaH_2PO_4 and Na_2HPO_4 in doubly distilled water (DDW, resistivity $>18\ M\Omega$ cm), and the pH value was adjusted to 7.4 by adding H_3PO_4 and NaOH. All chemicals used were of analytical grade unless otherwise stated.

2.2. Apparatus

A sensing scheme with two (dual) ceramic resonators connected in parallel was applied based on our previous study (Su et al., 2013). Two 40 MHz ceramic resonators (separated by at least 100 KHz) were connected in parallel and placed in a shielding metal box for frequency measurement at the same time, in which one resonator was used as the sensing unit and the other as the control unit. The ceramic resonators had gold plated electrodes ($0.39\ mm^2$) on both sides. The integrity of the electrode surface was inspected by scanning electron microscope (XL30 ESEM FEG, Philips Electron Optics, Netherlands).

2.3. Electrochemical measurements

The electrochemical experiments were carried out on a CHI660c potentiostat (CH Instruments Inc., Shanghai, China) in a conventional three-electrode system. The sensor chip served as a working electrode, an Ag/AgCl electrode was used as the reference electrode, and a platinum wire was the counter electrode. The electrodeposition was performed by cyclic voltammetric scanning in a 0.1 M PBS (pH 7.4) containing 2 mM $HAuCl_4$ from -1.25 V to -0.7 V for different cycles (1, 2, 5 and 10 cycles, designed as 1-, 2-, 5- and 10-cycle) at a scan rate of 50 mV/s, and the surface area evaluation of electrodes was conducted by cyclic voltammetric scanning in a solution of $K_3[Fe(CN)_6]$ (1 mM) dissolved in 1 M KCl. Electrochemical impedance spectroscopy (EIS) measurements were performed in 1 M KCl containing 5 mM $K_4[Fe(CN)_6]$, and 5 mM $K_3[Fe(CN)_6$. The electrochemical impedance spectra were recorded within the frequency range of 100 kHz and 100 mHz. The amplitude of the applied sine wave potential was 5 mV.

2.4. Synthesis of thiolated-BPA and formation of self-assembled monolayer

The synthesis of the thiolated-BPA (SH-BPA) involved multi-step preparation under simple reaction conditions using the commercially available starting materials (Fig. 1a). 11-Mercaptoundecanoic acid (5 mM) was converted to a dimmer by the formation of a disulfide bond in a bromine-dichloromethane solution (6 mM in 10 ml CH_2Cl_2) at room temperature. After reaction for 10 min, the precipitate was collected and washed with cold dichloromethane (5 ml) for three times. The dimmer (4 mM) was further reacted with a *tert*-butyl (chloro)diphenylsilane protected bisphenol-A (9 mM) using the standard DCC (carbodiimide) coupling method (Hassner and Alexanian, 1978) in a dichloromethane solution at room temperature. The compound was then purified and isolated by flash column chromatography. The protecting group on the BPA was then removed by tetra-butylammonium fluoride (10 equivalents) in an acetonitrile solution. The desired compound was obtained and characterized with high resolution mass spectrometer: Experimental (M+Na) $m/z=877.4538$; calc. $m/z=877.4512$. The compound could dissolve in an ethanol-water solution. By applying 1.5 μl of different ratios of probe vs. spacer (MCH) solution to a gold electrode surface for 2 h,

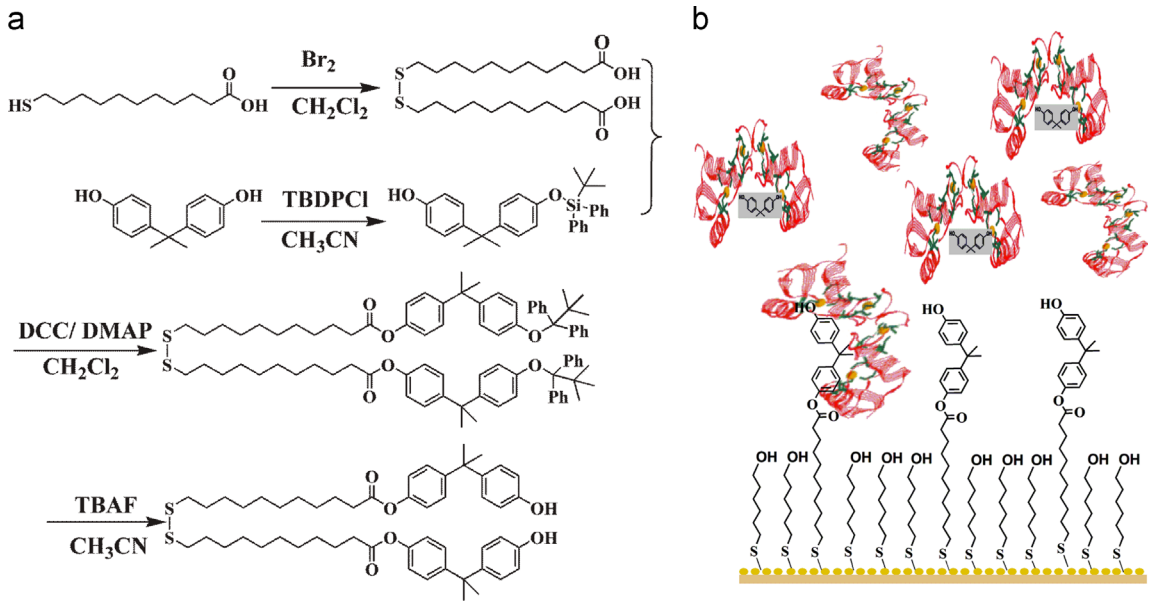

Fig. 1. The procedure of thiolated bisphenol A synthesis (a), and competitive binding assay for EDCs detection (b).

a self-assembled monolayer (SAM) with immobilized SH-BPA was prepared. MUD was employed to replace the SH-BPA for non-specific adsorption assay (control channel).

2.5. Binding of ER-α on SAM and detecting of EDCs using competitive binding assay

After a SAM with immobilized SH-BPA was prepared, different concentrations of ER-α at 0–35 nM were incubated with SAM/SH-BPA for 2 h. After washing away the unbounded protein, the frequency was measured and a linear ER-α binding curve was obtained. For competitive detection of EDCs (E1, E2 and BPA), different concentrations of E1, E2 and BPA were incubated with a fixed concentration of ER-α for 2 h. Then 1.5 μl of pre-incubated solution was added on the SAM for 2 h, where the un-reacted ER-α would bind to the SAM/SH-BPA. After complete rinsing the unbounded ER-α/EDCs, the frequency change upon different EDCs for the competitive assay were examined.

The specificity of the biosensor was studied using three kinds of environmental pollutants, including HDQ, 2-BRP and PBDE-47. 20 nM of these compounds (HDQ, 2-BRP and PBDE-47) or 10 nM EDCs (E1, E2 and BPA) were incubated with 30 nM ER-α for 2 h, respectively. Then 1.5 μl of incubated solution was added on the SAM for 2 h, and the frequency changes were measured after complete rinsing of the unbounded mixtures.

To investigate the utility of this ceramic biosensor for environmental sample analysis, 5 nM of E1, E2 or BPA, the general level of EDCs concentration found in surface waters, was spiked into tap water (pH 7.6) and seawater (pH 7.8) to estimate the recovery rate.

3. Results and discussion

3.1. Design of the piezoelectric biosensor for EDCs

The PZT piezoelectric biosensor was integrated with a competitive binding assay for the detection of EDCs. The sensor surface was first modified with Au nanoparticles (NPs) to increase the surface area and enhance binding capacity. To design the sensing interface of the biosensor, thiol-labeled long chain hydrocarbon conjugated with BPA as head group (Fig. 1a) was synthesized and self-assembled on the Au surface as the sensing probes. The sensing mechanism was based on the binding capacity of ER-α to the thiol-labeled BPA immobilized on the sensor surface in the presence of E1, E2 and BPA in the format of a competitive binding assay (Fig. 1b). Different concentrations of EDCs were incubated with optimized concentration of ER-α, and the unbounded ER-α was detected by the biosensor. The sensor signal was generated by monitoring the frequency change before and after the immune-reaction.

3.2. Modification and characterization of the gold NPs layer

Various types of NPs have been successfully used in analytical and electrochemical applications. Nanostructure modified electrodes often exhibit significantly enhanced active area for attaching probe molecules and improved electrochemical properties (Wang et al., 2013a, 2013b; Yi et al., 2013; Zhang et al., 2009). For examples, biosensors modified with Au NPs (Lin et al., 2012; Zhen et al., 2012), magnetic NPs (Chuah et al., 2012; Wang et al., 2010; Zhang et al., 2007) or conducting polymer nanomaterials (Choong and Milne, 2010; Gerard et al., 2002; Wang et al., 2013a) have shown greatly improved detection sensitivity.

To enlarge the surface area and enhance the binding capacity of the biosensor, we modified the sensor electrodes with different-sized Au NPs by a facile electrodeposition (Ma et al., 2009) with different cyclic voltammetric scan cycles. Fig. 2 depicts the typically scanning electron microscopy (SEM) images of the original (bare) electrode (Fig. 2a) and the Au NPs modified electrodes (Fig. 2b–e), respectively. As shown in the images, a remarkable feature is that the surface of the original electrode was scraggly and smooth (Fig. 2a), while the surface of the modified electrode was coated with a layer of uniform NPs (Fig. 2b–e). The sizes of the NPs on the modified electrode increased from ~15 nm (1-cycle), to ~25 nm (2-cycle), ~50 nm (5-cycle), and ~65 nm (10-cycle) as shown in the enlarged SEM images (insets of Fig. 2b–e).

3.3. Electrochemical characterization of the modified electrodes

The surface areas of the electrodes were evaluated by an electrochemical method. Fig. 3a shows the cyclic voltammetry response of the bare and modified electrodes in 1 M KCl solution

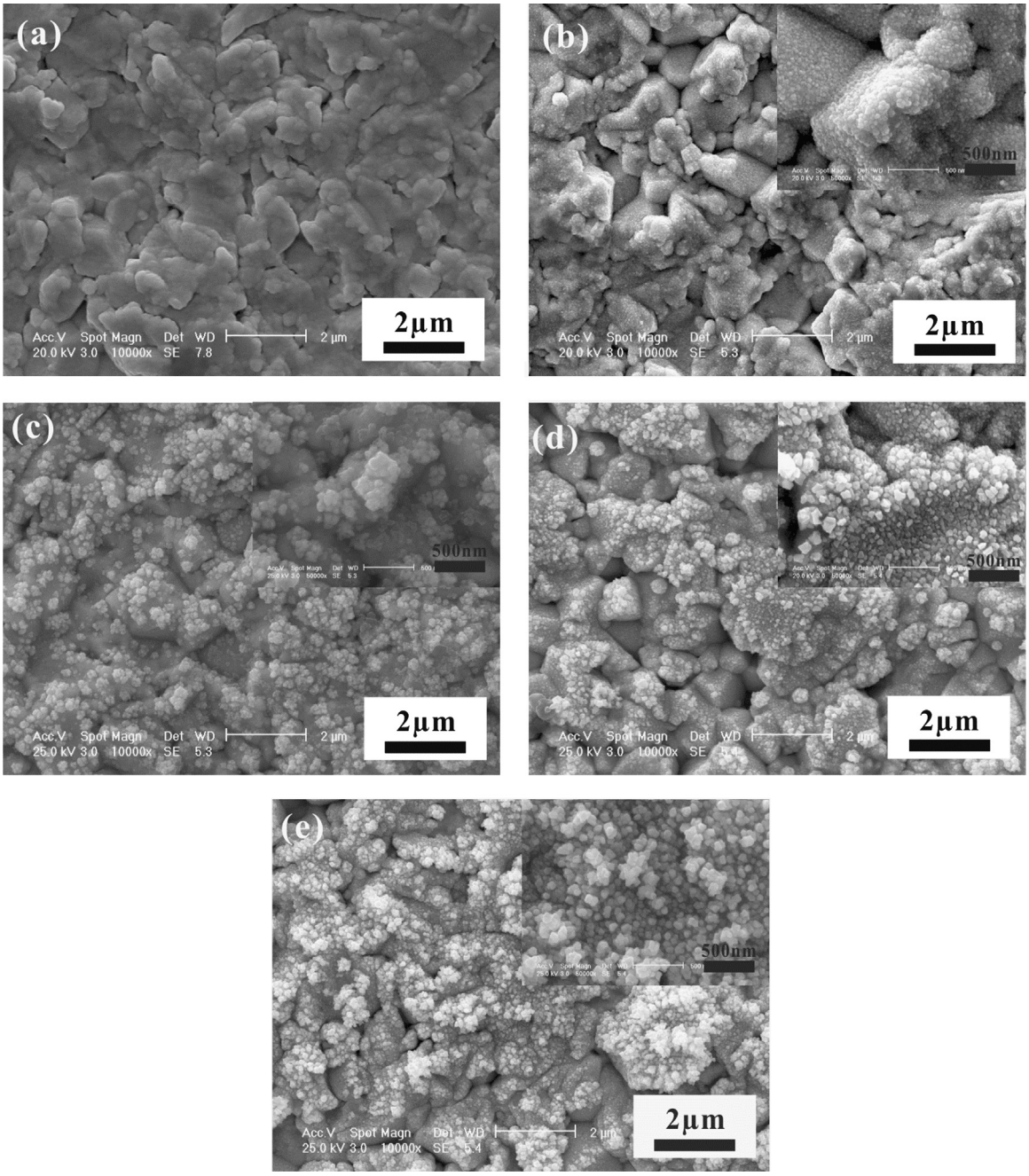

Fig. 2. SEM images of bare electrode (a) and Au NPs modified electrodes (b–e). The insets in (b–e) are the enlarged image of modified electrodes.

containing 1 mM $K_3[Fe(CN)_6]$ at a scan rate of 100 mV s^{-1}. The actual areas of the electrodes can be estimated according to the Randles–Sevcik equation (Bard and Faulker, 2001):

$$I_p = 2.69 \times 10^5 n^{3/2} A D_0^{1/2} c_0 v^{1/2}$$

in which I_p, n, A, D_0, C_0, and v represent the redox peak current (A), the number of electrons per molecule oxidized or reduced ($n=1$), the electrode surface area (cm^2), the diffusion coefficient of $K_3[Fe(CN)_6]$ in 1 M KCl (7.6×10^{-6} cm^2 s^{-1}) (Tang et al., 2009), the concentration of redox species (mol cm^{-3}), and the scan rate (V s^{-1}), respectively. The peak current increased gradually from 6.1×10^{-7} A at the bare electrode (Fig. 3a, 0-cycle) to 6.7×10^{-7} A (1-cycle), 7.4×10^{-7} A (2-cycle) and 8.3×10^{-7} A (5-cycle) at Au NPs modified electrodes, respectively, and rose slightly at the modified electrode with 10 scanning cycles. The real surface areas of the bare and Au NPs coated electrodes (5-cycle) calculated according to the equation were 0.52 and 0.71 mm^2, respectively, which means the surface area of the modified electrode was enlarged by 1.4 times. Besides, the actual surface area (0.52 mm^2) of the bare electrode is larger than the geometric area (0.39 mm^2) because of surface roughness of the gold plated electrode (Fig. 2a). As the surface area of Au NPs modified electrode do not increase after 5 cycles scanning deposition, the 5-cycle electrodes were used to study further.

Electrochemical impedance spectroscopy (EIS) has been used as an effective laboratory-based research tool for probing the features and performance of chemically-modified electrodes. In EIS, the semicircle portion observed at high frequencies corresponds to the charge transfer resistance (R_{ct}). The parameter R_{ct} was obtained by fitting the impedance spectra to the Randles equivalent circuit as illustrated in Fig. 3b (inset). In the presence of

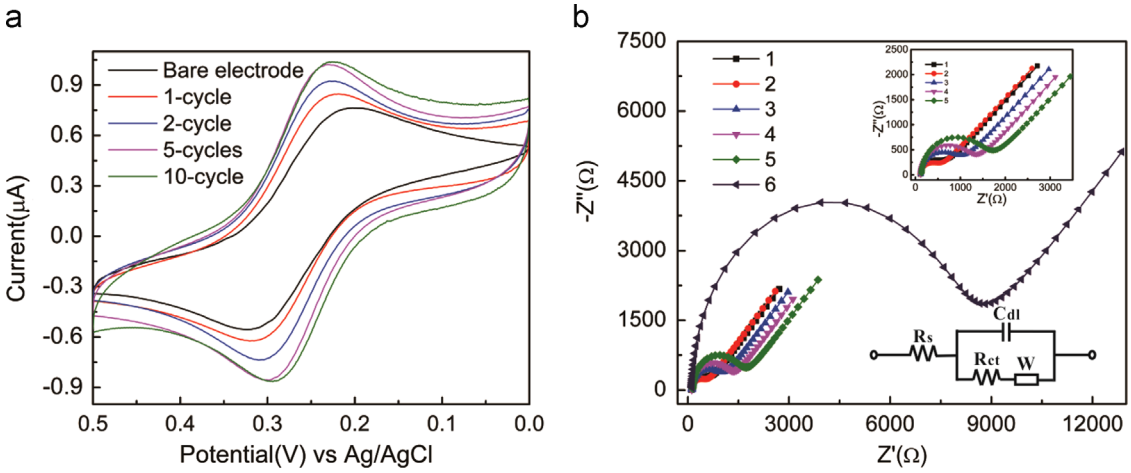

Fig. 3. (a) Cyclic voltammetric profiles acquired from the bare electrode and modified electrodes (1-, 2-, 5- and 10-cycle) in 1 M KCl solution containing 1 mM $K_3[Fe(CN)_6]$ at a scan rate of 100 mV/s. (b) Nyquist diagram of EIS recorded from 100 kHz and 100 mHz for $[Fe(CN)_6]^{3-}/[Fe(CN)_6]^{4-}$ (5 mM, 1:1) in 1.0 M KCl at bare electrode (curve 1), Au NPs modified electrode (curve 2), SAM (MCH/MUD, curve 3; MCH/SH-BPA, curve 4) coated electrodes, ER-α bound electrodes (bound to the MCH/MUD, curve 5; bound to the MCH/SH-BPA, curve 6). The inset represents the Randles equivalent circuit model.

redox probe ($[Fe(CN)_6]^{3-}/[Fe(CN)_6]^{4-}$), the resistance of surface R_{ct} was affected by the electrodeposition Au NPs, the modification with SAMs (MCH/MUD, MCH/SH-BPA), and also the binding with ER-α (Fig. 3b). Before modification, R_{ct} of the bare electrode was about 715 Ω (Fig. 3b, curve 1). The addition of Au NPs on the electrode gave a lower resistance of around 618 Ω (Fig. 3b, curve 2), because the excellent electrochemical properties of Au NPs facilitated the electron transfer process. After SAMs of MCH/MUD and MCH/SH-BPA were assembled on the Au NPs modified electrodes, the resistance increased to 1283 Ω and 1475 Ω, respectively. Finally, after incubating 1.5 μl of 25 nM ER-α with the SAM, the R_{ct} obtained from both SAMs increased, but the value on MCH/SH-BPA (9565 Ω, Fig. 3b, curve 6) was much greater than that on MCH/MUD (1817 Ω, Fig. 3b, curve 5), suggesting that ER-α molecules were bound to the specific probes (SH-BPA) and blocked the electron exchange between the redox probe and the electrode (Fig. 3b, curve 6).

3.4. Optimizing the mixed SAM layer and binding of ER-α to SH-BPA on SAM

For specific sample detection, a dual sensor chip was used. One was modified with SH-BPA conjugated SAM as specific probes and the other was coated with SAM of MUD (with the same length of hydrocarbon chain as the probe) as control channel to measure non-specific adsorption. To investigate the ER-α binding capacity of the mixed SAMs, different ratios of probe (0.5, 1.0, 2.0, 5.0 and 10.0%) over spacer (MCH) were self-assembled on sensor surface for 2 h. After washing, ER-α at 25 nM was incubated with the SAM layer for 2 h, and the frequency was measured after washing away the unbound ER-α. As shown in Fig. 4a, the frequency change (Δf) increased with the percentages of probe from 0.5% to 2.0% before decreased with higher ratios of the probe. 2.0% molar ratio of the probe showed the highest ER-α binding capacity. This is probably due to steric hindrance (Jung et al., 2000; Deng et al., 2006) on the SAM with high ratios of probe, which is unfavorable to the binding of ER-α to the SAM. The frequency changes at Au NPs modified sensor were much larger than the bare electrode (without Au NPs modification), since the Au NPs increased the surface area and enhanced the binding capacity of the immobilizing probes (Saha et al., 2012). To optimize the incubation time, 25 nM ER-α was incubated with SAM/SH-BPA from 0.5 to 5 h, and the frequency was tested after washing the unbound ER-α. The results suggested that an incubating time of 2 h could lead to the binding saturation (Supplemental, Fig. S1).

As described above, the mixtures with the ratio of 2.0% probe or MUD over spacer were self-assembled on sensor electrodes. Then, different concentrations of ER-α from 0 to 35 nM were incubated with SAM/SH-BPA or control SAM/MUD for 2 h, and the frequency was measured after removing the unbound protein (Fig. 4b). The frequency changes increased linearly with the concentration of ER-α from 1 nM to 30 nM on the SAM/SH-BPA and with a correlation coefficient of 0.9703. Although non-specific adsorption on the SAM/MUD surface was also observed to be proportional to the concentration of ER-α, the changes were nonetheless much lower than the specific binding on the SAM/SH-BPA sensor, indicating that the SH-BPA probe enhanced the binding capacity of the sensor surface for ER-α. In addition, to test the specific/non-specific adsorption of the SAM/SH-BPA, the same concentrations (0–35 nM) of BSA (BSA has similar molecular weight to ER-α) were used to incubate on the SAM/SH-BPA sensor surface. The data showed that the BSA adsorption on the sensor layer is similar to the non-specific adsorption of ER-α on the SAM/MUD surface (Supplemental, Fig. S2), which confirmed the specificity of the developed sensor probe for ER-α binding.

Adsorption of proteins at surfaces of self-assembled organic monolayers (SAM) is a complex process; different SAMs may induce different extents of protein adsorption (Prime and Whitesides, 1991; Abramov et al., 2004; Jin et al., 2009). The basic mechanism of protein adsorption is dependent on the nature of the protein itself, the medium in which it is positioned, and the nature of the SAM surface (Andrade, 1985; Masson et al., 2006). Proteins have hydrophobic, ionic, and polar domains, and protein adsorption to SAM surfaces is common, since the surface of SAM also exhibits hydrophobic, ionic, or polar properties. The non-specific adsorption of ER-α protein on the sensor surface observed in this study is relatively high, which is probably due to the much longer length of the probes than the spacers, because the heterogeneous lengths increased accessibility of protein to the sensor surface as previously reported (Mittler-Neher et al., 1995; Patel et al., 1998; Choi et al., 2005).

There are a number of methods that may be used to reduce non-specific protein adsorption, which will be the subject of subsequent study. For example, poly(ethylene

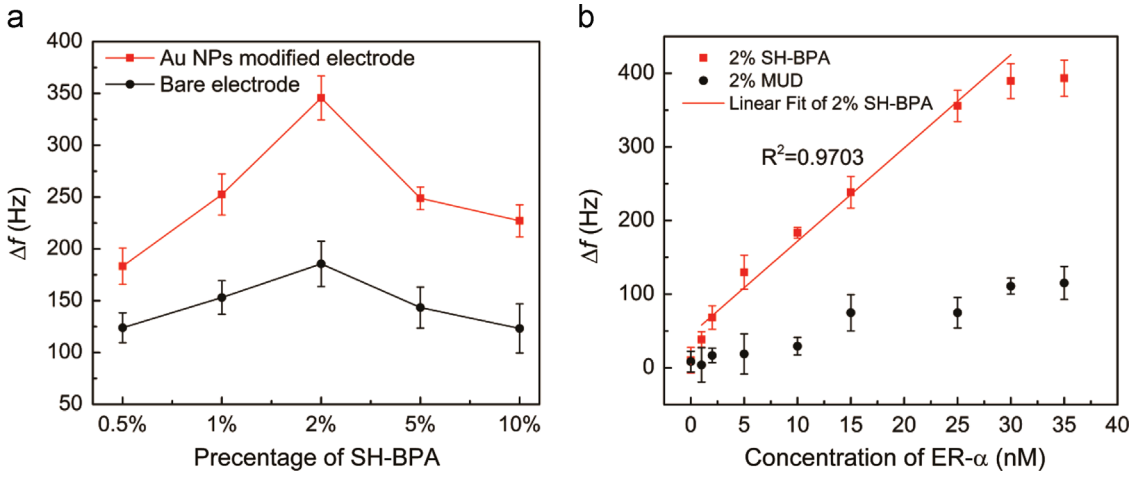

Fig. 4. (a) Optimization of probe and spacer molar ratio for ER-α binding at 25 nM and (b) binding assay of different concentrations (from 0 to 35 nM) of ER-α to MCH/SH-BPA.

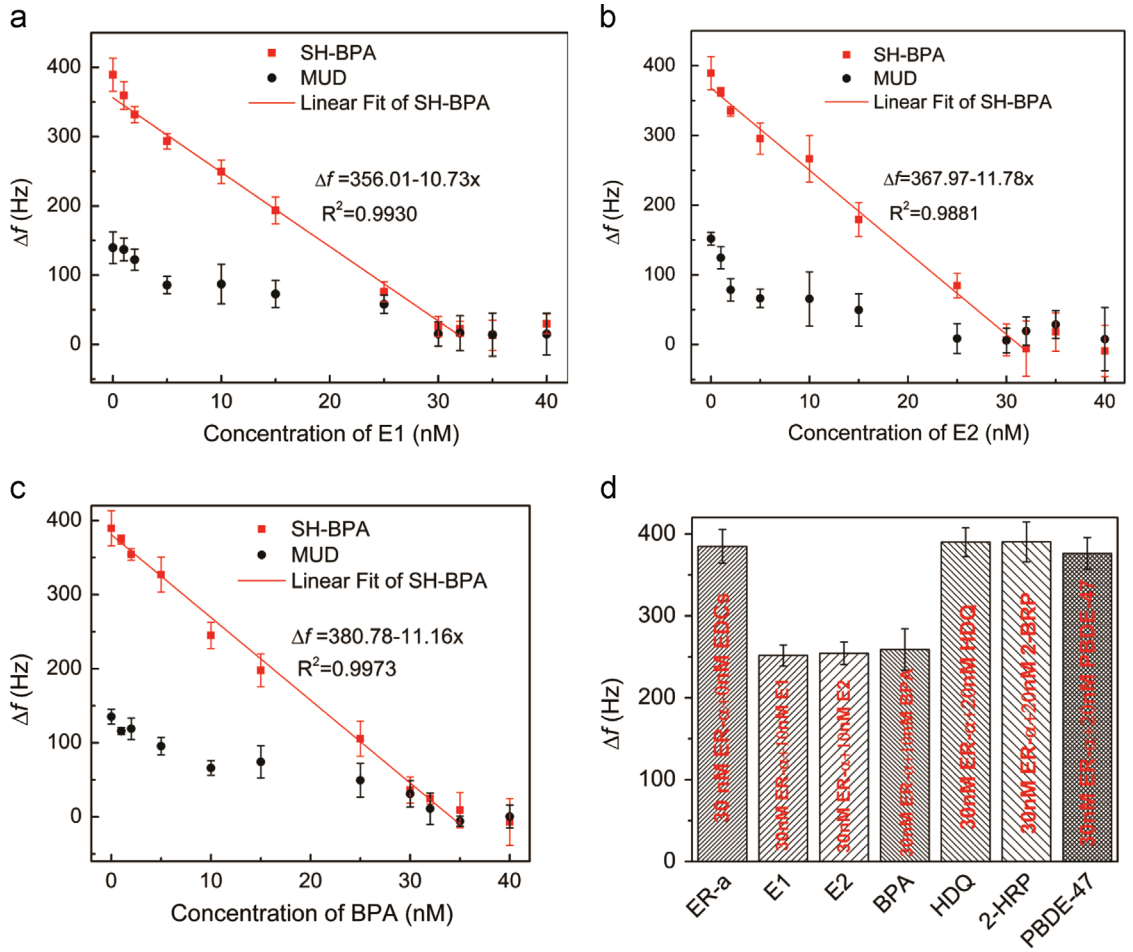

Fig. 5. Competitive binding assay for E1 (a), E2 (b) and BPA (c) detection. (d) The specificity of the biosensor was verified by the response to three non-specific environmental pollutants (HDQ, 2-BRP and PBDE-47).

glycol)-terminated thiols (such as carboxyl-PEG12-thiol) may be employed to replace the spacer alkanethiols to resist proteins adsorption on the SAM (Prime and Whitesides, 1991; Wang and Kreuzer, 1997). In addition, N-hydroxysuccinimide ester alkanethiols have been reported to have the ability to reduce proteins adsorption on the SAM (Frederix et al., 2004). Furthermore, by attaching amino acids to alkanethiols for the formation of SAM, non-specific adsorption of proteins from solution may be limited (Chapman et al., 2000).

3.5. Detection of EDCs by competitive binding assay

Most of the EDCs are small molecules and difficult to be detected directly by a piezoelectric sensor. Therefore, a competitive binding

Table 1
Recovery of spiked EDCs in natural water ($n=3$).

	Tap water				Seawater			
	Spike level (nM)	Determined level (nM)	Recovery (%)	RSD (%)	Spike level (nM)	Determined level (nM)	Recovery (%)	RSD (%)
E1	5.0	5.07	101.4	5.6	5.0	5.32	106.4	6.8
E2	5.0	4.73	94.7	6.0	5.0	5.39	107.8	4.8
BPA	5.0	5.13	102.6	4.7	5.0	5.49	109.8	3.1

assay was integrated to indirectly determine these compounds. Firstly, the optimum amount of ER-α (30 nM) was used to incubate with various concentrations of E1, E2 or BPA (0–40 nM) for 2 h. Then, by assaying the free ER-α of the incubated solution, the concentrations of E1, E2 and BPA could be calculated. The frequency changes upon different E1, E2 and BPA concentrations for the competitive biosensor assay could be used to construct the standard curves. Fig. 5 depicts the frequency changes upon the binding of free ER-α to the sensor surface modified with SAM/SH-BPA in the presence of EDCs. The result showed that frequency shifts were minimal at control channel (SAM/MUD), while specific probe binding resulted in significant frequency changes with only small amount of samples required (1.5 μl). As shown in Fig. 5a–c, the higher concentration of EDCs in the solution the less free ER-α remained in the incubated solution. The frequency changes decreased with increasing concentration of E1 (Fig. 5a), E2 (Fig. 5b) and BPA (Fig. 5c), respectively. The linear detection ranges of E1, E2 and BPA were 1–32 nM (with a correlation coefficient of 0.9930), 1–32 nM (with a correlation coefficient of 0.9807), and 1–35 nM (with a correlation coefficient of 0.9973), respectively. The detection limits of ($S/N=3$) E1, E2 and BPA were calculated to be 2.4 nM (0.65 ng/ml), 2.6 nM (0.71 ng/ml) and 2.9 nM (0.66 ng/ml), respectively, which are lower than or comparable to values from the literature (Mei et al., 2013; Piao et al., 2008; Rahman et al., 2007; Wu et al., 2012; Xu et al., 2012).

3.6. Biosensor specificity and application to environmental water samples

The specificity of the biosensor was tested by incubating with 20 nM of three types of environmental pollutants (including HDQ, 2-BRP and PBDE-47) or 10 nM EDCs (E1, E2 and BPA) with 30 nM ER-α for 2 h, respectively, followed by measuring the amount of the free ER-α in the incubated solution. As illustrated in Fig. 5d, obvious decrease of frequency changes observed in the presence of EDCs, while there were no decreases in the presence of other types of environmental pollutants, indicating the biosensor has a good specificity for EDCs detection.

To further validate the accuracy and application of the developed method, we spiked 5 nM of E1, E2 and BPA, the general concentration level of EDCs found in surface waters, into tap water (pH 7.6) and seawater (pH 7.8) and conducted the recovery experiments. Both the tap water and seawater samples were filtered through a 0.22 μm membrane filter. Table 1 tabulated the performance of the analytical method on the various sample matrices. The recoveries of E1, E2 and BPA from tap water were in the range from 94.7% to 102.6%, and the values from seawater were 106.4–109.8%. The results confirmed that this biosensor assay would be a useful screening test for EDCs residues in environmental samples. The relative standard deviations (RSD) are $<6.8\%$ for 3 successive assays. This result is comparable to other methods (Meesters and Schroder, 2002; Mei et al., 2013; Piao et al., 2008; Tschmelak et al., 2004; Xu et al., 2012), where the recoveries of EDCs were found in the range between 92.0% and 110.0%.

4. Conclusion

A novel piezoelectric ceramic biosensor for label-free, low cost, and direct detection of EDCs was developed. A thiolated-BPA was synthesized and self-assembled on Au NPs modified ceramic sensor surface as a specific probe for detecting E1, E2 and BPA through a competitive binding assay. The piezoelectric ceramic biosensor exhibited excellent sensitivity, good reproducibility and specificity towards the quantification of EDCs using a small volume of sample (1.5 μl), with wide linear range and fast assay time. The piezoelectric ceramic biosensor platform may be used for rapid and sensitive detection of EDCs in environmental samples, and further research will focus on reducing non-specific adsorption and utilizing the miniaturized size of the ceramic resonators to develop sensor arrays for multiplex detection.

Acknowledgments

This study was supported by grants from the Shenzhen Key Laboratory Funding Scheme of Shenzhen Municipal Government, the National Key Scientific Research Program (973 Program No. 2012CB933302), the University Grants Committee of Hong Kong (AoE/P-04/04), and the General Research Fund (CityU-103312). We thank Murata Manufacturing Co. Ltd. (Kyoto, Japan) for providing ceramic resonators and technical support.

Appendix A. Supplementary material

Supplementary data associated with this article can be found in the online version at http://dx.doi.org/10.1016/j.bios.2013.09.068.

References

Abramov, M.A., Dehaen, W., Maes, G.J., 2004. Journal of Biochemical and Biophysical Methods 58 (1), 67–74.
Andrade, J., 1985. Surface and Interfacial Aspects of Biomedical Polymers. Plenum, New York.
Ahmed, S., Owen, C.P., James, K., Sampson, L., Patel, C.K., 2002. Current Medicinal Chemistry 9 (2), 263–273.
Ash, M., Ash, I., 2005. Handbook of Plastic and Rubber Additives. Synapse Information Resources, Inc.
Bard, A.J., Faulker, L.R., 2001. Electrochemical Methods: Fundamentals and Applications, 2nd ed. Wiley, New York.
Chapman, R.G., Ostuni, E., Yan, L., Whitesides, G.M., 2000. Langmuir 16 (17), 6927–6936.
Choi, S.H., Lee, J.W., Sim, S.J., 2005. Biosensors and Bioelectronics 21 (2), 378–383.
Choong, C.L., Milne, W.I., 2010. Biosensors and Bioelectronics 25 (10), 2384–2388.
Chuah, K., Lai, L.M., Goon, I.Y., Parker, S.G., Amal, R., Justin Gooding, J., 2012. Chemical Communications 48 (29), 3503–3505.
Colborn, T., Saal, F.S.V., Soto, A.M., 1993. Environmental Health Perspectives 101 (5), 378–384.
D'Antuono, A., Dall'Orto, V.C., Lo Balbo, A., Sobral, S., Rezzano, I., 2001. Journal of Agricultural and Food Chemistry 49 (3), 1098–1101.
Damgaard, I.N., Main, K.M., Toppari, J., Skakkebaek, N.E., 2002. Best Practice and Research Clinical Endocrinology and Metabolism 16 (2), 289–309.
Delbes, G., Levacher, C., Habert, R., 2006. Reproduction 132 (4), 527–538.

Di Carro, M., Scapolla, C., Liscio, C., Magi, E., 2010. Analytical and Bioanalytical Chemistry 398 (2), 1025–1034.
Deng, T., Li, J.S., Huan, S.Y., Yang, H.F., Wang, H., Shen, G.L., Yu, R.Q., 2006. Biosensors and Bioelectronics 21 (8), 1545–1552.
Diamanti-Kandarakis, E., Bourguignon, J.P., Giudice, L.C., Hauser, R., Prins, G.S., Soto, A.M., Zoeller, R.T., Gore, A.C., 2009. Endocrine Reviews 30 (4), 293–342.
Fang, H., Tong, W., Branham, W.S., Moland, C.L., Dial, S.L., Hong, H., Xie, Q., Perkins, R., Owens, W., Sheehan, D.M., 2003. Chemical Research in Toxicology 16 (10), 1338–1358.
Frederix, F., Bonroy, K., Reekmans, G., Laureyn, W., Campitelli, A., Abramov, M.A., Dehaen, W., Maes, G., 2004. Journal of Biochemical and Biophysical Methods 58 (1), 67–74.
Gerard, M., Chaubey, A., Malhotra, B.D., 2002. Biosensors and Bioelectronics 17 (5), 345–359.
Gomes, R.L., Lester, J.N., 2002. Endocrine Disrupters in Drinking Water and Water Reuse. In: Birkett, J.W., Lester, J.N. (Eds.), Endocrine Disruptors in Wastewater and Sludge Treatment Processes. CRC Press, London, pp. 177–218.
Gutierrez-Gallego, R., Bosch, J., Such-Sanmartin, G., Segura, J., 2009. Growth Hormone and IGF Research 19 (4), 388–398.
Hamid, H., Eskicioglu, C., 2012. Water Research 46 (18), 5813–5833.
Hassner, A., Alexanian, V., 1978. Tetrahedron Letters 19 (46), 4475–4478.
Jin, X.Y., Jin, X.F., Chen, L.G., Jiang, J.H., Shen, G.L., Yu, R.Q., 2009. Biosensors and Bioelectronics 24 (8), 2580–2585.
Jung, L.S., Nelson, K.E., Stayton, P.S., Campbell, C.T., 2000. Langmuir 16 (24), 9421–9432.
Krishnan, A.V., Stathis, P., Permuth, S.F., Tokes, L., Feldman, D., 1993. Endocrinology 132 (6), 2279–2286.
Lin, C.Y., Fuh, M.R., Huang, S.D., 2011. Journal of Separation Science 34 (4), 428–435.
Lin, D., Wu, J., Wang, M., Yan, F., Ju, H., 2012. Analytical Chemistry 84 (8), 3662–3668.
Liu, Z.H., Kanjo, Y., Mizutani, S., 2009. Science of the Total Environment 407 (18), 4975–4985.
Lu, J., Wu, J., Stoffella, P.J., Wilson, P.C., 2013. Journal of Agricultural and Food ChemistryFood Chemistry 61 (1), 84–89.
Ma, Y.T., Di, J.W., Yan, X., Zhao, M.L., Lu, Z.J., Tu, Y.F., 2009. Biosensors and Bioelectronics 24 (5), 1480–1483.
Magi, E., Scapolla, C., Di Carro, M., Liscio, C., 2010. Journal of Mass Spectrometry 45 (9), 1003–1011.
Marchesini, G.R., Meulenberg, E., Haasnoot, W., Irth, H., 2005. Analytica Chimica Acta 528 (1), 37–45.
Masson, J.F., Battaglia, T.M., Cramer, J., Beaudoin, S., Sierks, M., Booksh, K.S., 2006. Analytical and Bioanalytical Chemistry 386 (7–8), 1951–1959.
Matsumoto, K., Sakai, T., Torimaru, A., Ishitobi, S., 2005. Journal of the Faculty of Agriculture Kyushu University 50 (2), 625–634.
Matsunaga, T., Ueki, F., Obata, K., Tajima, H., Tanaka, T., Takeyama, H., Goda, Y., Fujimoto, S., 2003. Analytica Chimica Acta 475 (1–2), 75–83.
McLachlan, J.A., Simpson, E., Martin, M., 2006. Best Practice and Research Clinical Endocrinology and Metabolism 20 (1), 63–75.
Meesters, R.J.W., Schroder, H.F., 2002. Analytical Chemistry 74 (14), 3566–3574.
Mei, Z., Chu, H., Chen, W., Xue, F., Liu, J., Xu, H., Zhang, R., Zheng, L., 2013. Biosensors and Bioelectronics 39 (1), 26–30.
Mittler-Neher, S., Spinke, J., Liley, M., Nelles, G., Weisser, M., Bace, R., Wenz, G., Knoll, W., 1995. Biosensors and Bioelectronics 10 (9–10), 903–916.
Patel, N., Davies, M.C., Heaton, R.J., Roberts, C.J., Tendler, S.J.B., Williams, P.M., 1998. Applied Physics A 66 (1), S569–S574.
Patil, S.H., Banerjee, K., Utture, S.C., Fontana, A.R., Altamirano, J.C., Oulkar, D.P., Wagh, S.S., Dasgupta, S., Patil, S.B., Jadhav, M.R., Ugare, B.R., Adsule, P.G., Deshmukh, M.B., 2011. Food Chemistry 124 (4), 1734–1740.
Piao, M.H., Noh, H.B., Rahman, M.A., Won, M.S., Shim, Y.B., 2008. Electroanal 20 (1), 30–37.
Prime, K.L., Whitesides, G.M., 1991. Science 252 (5009), 1164–1167.
Rahman, M.A., Shiddiky, M.J., Park, J.S., Shim, Y.B., 2007. Biosensors and Bioelectronics 22 (11), 2464–2470.
Rodriguez-Mozaz, S., de Alda, M.L., Barcelo, D., 2005. Water Research 39 (20), 5071–5079.
Saha, K., Agasti, S.S., Kim, C., Li, X.N., Rotello, V.M., 2012. Chemical Reviews 112 (5), 2739–2779.
Su, L., Zou, L., Fong, C.C., Wong, W.L., Wei, F., Wong, K.Y., Wu, R.S., Yang, M., 2013. Biosensors and Bioelectronics 46, 155–161.
Tabb, M.M., Blumberg, B., 2006. Molecular Endocrinology 20 (3), 475–482.
Tanaka, T., Takeda, H., Ueki, F., Obata, K., Tajima, H., Takeyama, H., Goda, Y., Fujimoto, S., Matsunaga, T., 2004. Journal of Biotechnology 108 (2), 153–159.
Tang, L.H., Wang, Y., Li, Y.M., Feng, H.B., Lu, J., Li, J.H., 2009. Advanced Functional Materials 19 (17), 2782–2789.
Tschmelak, J., Proll, G., Gauglitz, G., 2004. Biosensors and Bioelectronics 20 (4), 743–752.
Tsutsumi, O., 2005. Journal of Steroid Biochemistry and Molecular Biology 93 (2–5), 325–330.
Vandenberg, L.N., Hauser, R., Marcus, M., Olea, N., Welshons, W.V., 2007. Reproductive Toxicology 24 (2), 139–177.
Vandenberg, L.N., Chahoud, I., Heindel, J.J., Padmanabhan, V., Paumgartten, F.J., Schoenfelder, G., 2010. Environmental Health Perspectives 118 (8), 1055–1070.
Wang, J., Munir, A., Zhu, Z., Zhou, H.S., 2010. Analytical Chemistry 82 (16), 6782–6789.
Wang, L., Wen, W., Xiong, H., Zhang, X., Gu, H., Wang, S., 2013a. Analytica Chimica Acta 758, 66–71.
Wang, R.L.C., Kreuzer, H.J., 1997. Journal of Physical Chemistry B 101 (47), 9767–9773.
Wang, S., Li, L., Jin, H.L., Yang, T., Bao, W.W., Huang, S.M., Wang, J.H., 2013b. Biosensors and Bioelectronics 41, 205–210.
Waring, R.H., Harris, R.M., 2005. Molecular and Cellular Endocrinology 244 (1–2), 2–9.
Wu, L.D., Deng, D.H., Jin, J., Lu, X.B., Chen, J.P., 2012. Biosensors and Bioelectronics 35 (1), 193–199.
Xu, Z., Kuang, H., Yan, W.J., Hao, C.L., Xing, C.R., Wu, X.L., Wang, L.B., Xu, C.L., 2012. Biosensors and Bioelectronics 32 (1), 183–187.
Yi, Z., Li, X.Y., Liu, F.J., Jin, P.Y., Chu, X., Yu, R.Q., 2013. Biosensors and Bioelectronics 43, 308–314.
Zhang, X., Su, H., Bi, S., Li, S., Zhang, S., 2009. Biosensors and Bioelectronics 24 (8), 2730–2734.
Zhang, Y., Zeng, G.M., Tang, L., Huang, D.L., Jiang, X.Y., Chen, Y.N., 2007. Biosensors and Bioelectronics 22 (9–10), 2121–2126.
Zhen, Z., Tang, L.J., Long, H., Jiang, J.H., 2012. Analytical Chemistry 84 (8), 3614–3620.